Acta Cryst. (1950). **3**, 341

The Crystal Structure of Tartaric Acid

BY F. STERN AND C. A. BEEVERS

Dewar Crystallographic Laboratory, University of Edinburgh, Scotland

(*Received* 17 *February* 1950)

The structure of the optically active form of tartaric acid has been determined by Patterson and Fourier methods.

The molecule is found to have essentially the same configuration as the tartrate ion in Rochelle salt, containing two planar =C.OH.COOH groups inclined to each other at an angle of about 63°. Molecules are linked to each other by hydrogen bonds which show a strong tendency to lie in the planes of the flat =C.OH.COOH groups.

Introduction

The structure of tartaric acid, has been of interest since the time of Pasteur's work on enantiomorphism and molecular dissymmetry. In X-ray crystallographic technique its analysis affords a good example of the application of three-dimensional Patterson methods to structures of low symmetry containing no heavy atoms.

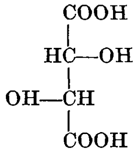

$$\begin{array}{c} \mathrm{COOH} \\ | \\ \mathrm{HC{-}OH} \\ | \\ \mathrm{OH{-}CH} \\ | \\ \mathrm{COOH} \end{array}$$

The unit cell and space group of tartaric acid have been determined by Astbury (1923) and by Reis & Schneider (1928). Astbury also put forward a structure suggested by the unit-cell size and symmetry and Bragg's atomic radii. This structure does not, however, agree with the configuration of the tartrate ion in Rochelle salt as determined at a later date by Beevers & Hughes (1941), and it is inconsistent with more extensive X-ray intensity data obtained from crystals of *d*-tartaric acid itself.

A preliminary account of this work has already been published (Beevers & Stern, 1948). In the present paper we shall describe the method of analysis and give more accurate values of the unit-cell dimensions and atomic parameters.

Crystal data

The morphology and optical properties of crystals of *d*-(*l*-)tartaric acid have been described by Groth (1906–19, vol. 3, p. 302) and Winchell (1943, p. 37).

Crystal class: monoclinic sphenoidal.

$$a:b:c = 1{\cdot}275:1:1{\cdot}027, \quad \beta = 100^\circ\, 17'.$$

Perfect cleavage along (100).

Molecular weight: 150·1. Density: 1·760 g.cm.$^{-3}$.

Refractive indices: $\alpha = 1{\cdot}496$, $\beta = 1{\cdot}535$, $\gamma = 1{\cdot}605$.

The unit-cell dimensions obtained from moving film photographs are

$$a = 7{\cdot}72 \pm 0{\cdot}02, \quad b = 6{\cdot}00 \pm 0{\cdot}02, \quad c = 6{\cdot}20 \pm 0{\cdot}02\,\text{A.};$$

$$\beta = 100^\circ\, 10' \pm 7',$$

giving $\quad a:b:c = 1{\cdot}287:1:1{\cdot}034.$

With the above values of density and molecular weight, and taking the number of molecules per mole $N = 6{\cdot}02 \times 10^{23}$, the number of molecules $C_4H_6O_6$ per unit cell is $1{\cdot}995 = 2$.

Systematic absences: (0*k*0) for *k* odd, hence the space group is $P2_1$.

The two molecules in the unit cell are thus related by a twofold screw axis parallel to the *b* axis and the structure is determined by 30 parameters, neglecting the hydrogen atoms.

Experimental: intensity measurements

Crystals were grown from an aqueous solution of *d*-tartaric acid and shaped into cylinders approximately 0·08 cm. in diameter and with their axes parallel to the three principal crystallographic axes.

All X-ray photographs were taken with copper $K\alpha$ radiation. The normal-beam Weissenberg technique was used to record the intensities which were estimated by visual comparison with a multiple-exposure oscillation strip.

After application of the usual correction factors the zero-layer intensities were reduced to the absolute scale using Wilson's method (Wilson, 1942), and later, during the final stages of the analysis, by comparison with the calculated intensities. The general intensities were reduced to the absolute scale by comparison with the corrected zero-layer intensities.

Interpretation of the Patterson function

Patterson projections along the *b* and *c* axes were first calculated and attempts were made to fit a model of the Patterson peaks of the tartrate molecule (as it occurs in Rochelle salt) to these projections. This, however, proved unsuccessful. Sections of the three-dimensional Patterson function were then computed at the levels $\quad y = 0, \quad y = \frac{1}{5} \quad$ and $\quad y = \frac{1}{2}$.

Harker (1936) has pointed out that certain regions of the three-dimensional Patterson function may contain peaks corresponding to the ends of vectors between atoms related by symmetry elements and thus be useful in finding the positions of such atoms. In the space group $P2_1$, for instance, there will be for every atom at (x,y,z) another equivalent one at $(\bar{x},\frac{1}{2}+y,\bar{z})$ related to the first by the twofold screw axis. This will give two peaks of the type $(2x,2z)$ in the $y=\frac{1}{2}$ Patterson section $P(x,\frac{1}{2},z)$. These peaks should enable the (x,z) coordinates of all the atoms to be determined apart from ambiguities (Buerger, 1946) which arise owing to the fact that a peak at $(2x,2z)$ in $P(x,\frac{1}{2},z)$ may be due to an atom in any one of the positions (x,z), $(x+\frac{1}{2},z)$, $(x,z+\frac{1}{2})$, $(x+\frac{1}{2},z+\frac{1}{2})$.

In the present case the interpretation of $P(x,\frac{1}{2},z)$ along these lines proved fruitless. The reason for this was seen on examining the $y=0$ Patterson section, $P(x,0,z)$. This latter strongly suggests that one of the $=$C.OH.COOH groups $C_2O_1C_3O_4O_5$ of the molecule lies in a plane perpendicular to the b axis. The group in its proper orientation, together with the peaks produced by it in $P(x,0,z)$, are shown in Fig. 1.

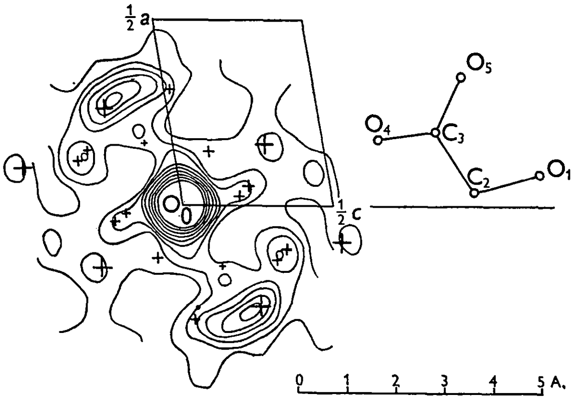

Fig. 1. Orientation of one of the $=$C.OH.COOH groups of the tartaric acid molecule compared with the central region of the $y=0$ Patterson section. Peaks due to atoms in this group are marked by crosses in the Patterson section, the sizes of the crosses indicating the relative weights of the peaks.

Two atoms at the same y level (x_1,y_0,z_1), (x_2,y_0,z_2), together with their equivalent atoms $(\bar{x}_1,y_0+\frac{1}{2},\bar{z}_1)$ and $(\bar{x}_2,y_0+\frac{1}{2},\bar{z}_2)$, will produce the following Patterson peaks:

(1) peaks of weight 1 at
$$(2x_1,\tfrac{1}{2},2z_1)$$
and at $$(2x_2,\tfrac{1}{2},2z_2),$$
(2) peaks of weight 2 at
$$(x_1-x_2,0,z_1-z_2)$$
(3) and at $$(x_1+x_2,\tfrac{1}{2},z_1+z_2),$$
(4) a peak of weight 4 at
$$(0,0,0).$$

Thus, in addition to the single-weight Harker peaks at $(2x_1,\frac{1}{2},2z_1)$ and $(2x_2,\frac{1}{2},2z_2)$ there occur in $P(x,\frac{1}{2},z)$ a double-weight peak at $(x_1+x_2,\frac{1}{2},z_1+z_2)$, i.e. situated halfway between the Harker peaks $(2x_1,\frac{1}{2},2z_1)$, $(2x_2,\frac{1}{2},2z_2)$.

The structure of tartaric acid was seen to have five atoms at the same y level, and its $P(x,\frac{1}{2},z)$ should, therefore, contain, in addition to their five Harker peaks, ten such double-weight peaks. It is the latter type of peak which will account for the main features of the $P(x,\frac{1}{2},z)$ synthesis.

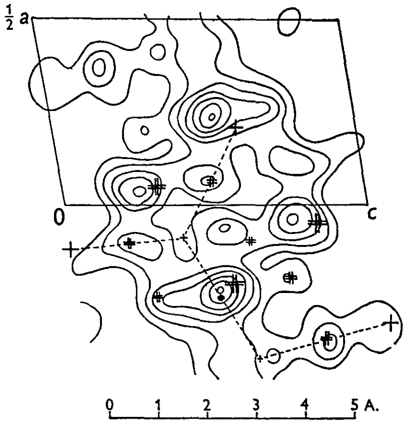

Fig. 2. Patterson section at $y=\frac{1}{2}$, together with the peaks at $y=\frac{1}{2}$ due to $C_2O_1C_3O_4O_5$, marked by crosses as in Fig. 1, double crosses indicating double-weight peaks. To estimate the quality of the agreement all crosses should be imagined as plotted on the asymmetric unit of the Patterson section.

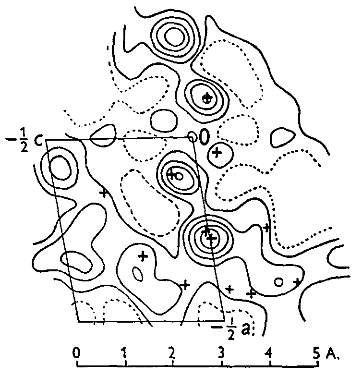

Fig. 3. Peaks in the $y=\frac{1}{5}$ Patterson section due to vectors between atoms belonging to the same molecule. Peaks are marked as in Fig. 1. To estimate the quality of the agreement all crosses should be imagined as plotted on the asymmetric unit of the Patterson section.

When the peaks of type (1) and (3) due to $C_2O_1C_3O_4O_5$ were plotted it was found that they could be fitted to the $(x,\frac{1}{2},z)$ synthesis *in only one position*, which is shown in Fig. 2. This fixed the position of the $=$C.OH.COOH group in the unit cell.

Since the distance of C_6 from the plane of $C_2O_1C_3O_4O_5$ is approximately 1·3 A. $(=\frac{1}{5}b)$, the $y=\frac{1}{5}$ Patterson section, $P(x,\frac{1}{5},z)$, can be expected to give information about the configuration of the other half of the molecule. If the molecule has the 'Rochelle salt configuration' (cf. Figs. 7 and 8), the $P(x,\frac{1}{5},z)$ section will contain peaks from $C_2O_1C_3O_4O_5$ to C_6 and C_8 together with the peak C_6–O_7 and, to a lesser extent, O_9–C_8, O_{10}–C_8. Peaks in the $P(x, \frac{1}{4}, z)$ section were observed in the expected positions (Fig. 3) confirming the postulated structure.

Fourier refinement

The approximate structure derived from the Patterson sections was refined by means of two-dimensional Fourier syntheses, giving projections of the electron density along the *b* and *c* axes. Of these the *b*-axis projection, containing a centre of symmetry, was by far the most useful in spite of a certain amount of overlapping of the atoms in the projection. Structure-factor charts were also used for this zone.

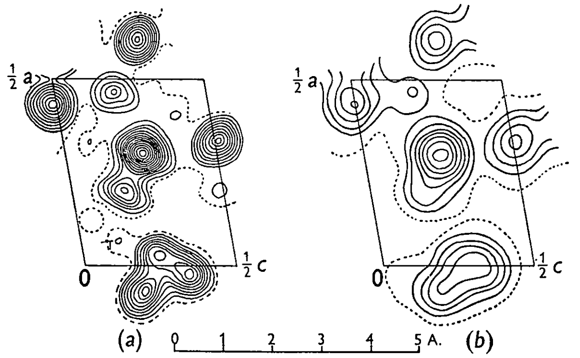

Fig. 4. Final *b*-axis Fourier projections (*a*) using absolute *F*'s, (*b*) using absolute *F*'s multiplied by $\exp(-2{\cdot}30 \sin^2 \theta)$. Contours are drawn at intervals of 2 e.A.$^{-2}$, the 2-electron contour being drawn dotted.

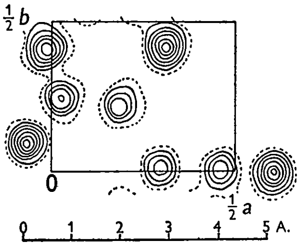

Fig. 5. Projection along the *c* axis of the unit-cell contents between the planes $z = 0{\cdot}100c$ and $z = 0{\cdot}417c$ showing all the atoms in the molecule except O_1 and O_4. Contours as in Fig. 4.

When the refinement by means of Fourier projections gave no further improvement, with

$$R = \frac{\Sigma\,||F_{\text{obs.}}| - |F_{\text{calc.}}||}{\Sigma\,|F_{\text{obs.}}|} = 0{\cdot}34,$$

the structure amplitudes for all the observed reflexions (about 600 in number) were calculated. The agreement with the observed *F*'s was fair, again giving $R = 0{\cdot}34$.

To get more reliable estimates of the *y* co-ordinates, and also of the *x*, *z* co-ordinates of atoms overlapping in the *b*-axis projection, a number of sections and bounded projections (Booth, 1945) were calculated using all observed *F*'s. The results were disappointing, probably owing to the absence of a centre of symmetry, and suggested few significant shifts of the atoms.

Final small adjustments of the structure were made from a *b*-axis Fourier projection with artificial temperature factor, $\exp(-2{\cdot}30 \sin^2 \theta)$. Examination of the tartaric acid molecule showed that the two —C.OH.COOH groups were planar except for C_8. Moving C_8 into the plane of $O_9O_{10}O_7C_6$ improved the agreement of the calculated and observed *F*'s and was therefore adopted.

The final *b*-axis Fourier projections without and with artificial temperature factor are shown in Fig. 4. Slices of the unit-cell contents containing the molecule (excluding O_1 and O_4) projected along the *c* axis are shown in Fig. 5. They can be compared with the drawing of the structure given in Fig. 8.

Apart from a possible inversion through the origin, which is discussed below, the table of atomic co-ordinates is as follows:

	x (A.)	*y* (A.)	*z* (A.)
O_1	2·57	0·08	3·16
O_4	3·32	5·94	6·11
O_5	4·68	5·92	1·86
O_7	2·41	2·48	1·56
O_9	7·26	0·52	1·13
O_{10}	7·59	2·38	2·07
C_2	2·24	0·02	1·67
C_3	3·54	0·02	1·14
C_6	1·61	1·26	1·06
C_8	0·26	1·44	1·55

Fig. 6 shows graphically the agreement of the observed and calculated *F*'s for the $F(0kl)$ $F(h0l)$ and $F(hk0)$ zones. The values of

$$R = \frac{\Sigma\,||F_{\text{obs.}}| - |F_{\text{calc.}}||}{\Sigma\,|F_{\text{obs.}}|}$$

for these zones are 0·26, 0·29 and 0·30 respectively. These relatively high values indicate that the structure is not sufficiently refined to render profitable a detailed examination of its accuracy, but it is considered that the co-ordinates are correct to within ±0·05 A.

Description of the structure

The molecule of tartaric acid has a general configuration identical with that found in Rochelle salt (Beevers & Hughes, 1941) as illustrated in Fig. 7. The carbon and oxygen atoms of each half —CH(OH).COOH of the molecule lie in a plane to within 0·07 A., the planes of the two halves making an angle of 63° ± 3° with each other. The interatomic distances within the molecule are as follows:

C_3–C_2 = 1·49 A. C_3–O_4 = 1·21 A.
C_2–C_6 = 1·47 C_3–O_5 = 1·24
C_6–C_8 = 1·53 C_8–O_9 = 1·20
C_2–$(OH)_1$ = 1·48 C_8–O_{10} = 1·17
C_6–$(OH)_7$ = 1·49

These distances are thought to be accurate to within ±0·05 A. The angles between the bonds in the molecule are shown in Fig. 7. The central carbon atoms, C_2 and

C_6, have bond angles which agree with the tetrahedral angle ($109\frac{1}{2}°$) except for the angle C_3–C_2–C_6, which is 102° and thus differs by more than 5° (our estimated probable error) from the tetrahedral angle. The O–C–O angles in both carboxyl groups are within a degree of 123°, which is the value in oxalic acid dihydrate (Robertson & Woodward, 1936; Dunitz & Robertson, 1947) and in β-succinic acid (Morrison & Robertson, 1949). The whole —COOH group is slightly rotated so that the two C–C–O angles are not equal, being approximately 126° and 110° respectively.

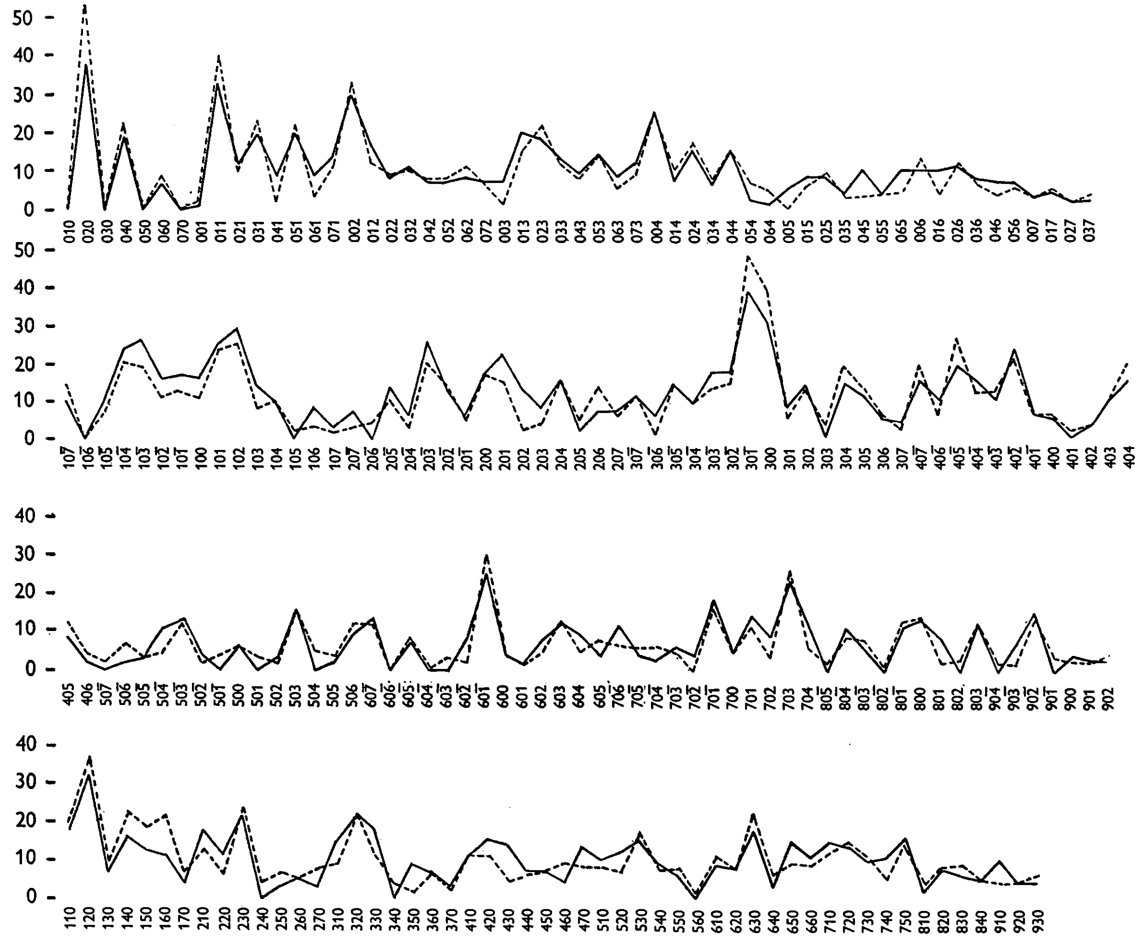

Fig. 6. Agreement of $F_{\text{calc.}}$ (shown by the broken line) and $F_{\text{obs.}}$ (shown by the full line) for the $F(0kl)$, $F(h0l)$ and $F(hk0)$ zones.

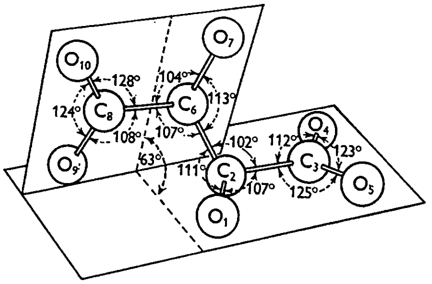

Fig. 7. Perspective drawing of the tartaric acid molecule showing the bond angles.

A diagram of the complete structure, projected down the *b* axis, is shown in Fig. 8, which covers four unit cells. Here the bonds within the molecule are represented by full lines, probable hydrogen bonds being shown by dotted lines. The dashed atoms are those derived from the others by the operation of the screw axis. The bonds linking the molecules are as follows:

O_4–O'_7 = 2·74 A.
O_5–O'_7 = 2·78
O_1–O'_{10} = 2·87
O_5–O_9 = 2·87
O_1–O_4 = 2·92

together with the five obtained by interchanging dashed and undashed atoms (i.e. operating by a screw axis). All other distances between oxygen atoms belonging to different molecules are greater than 3·00 A. The O_1–O_4 bond is the most doubtful one because of its greater length and since there are only four hydrogen atoms per molecule available for bonding. However, there seems in this structure to be no significant distinction between the =O and —OH bonds in the

—COOH groups, and it is possible that there is a statistical distribution of hydrogen atoms.

The configuration of the hydrogen bonds is of some interest. In Fig. 8 the half of the molecule, consisting of $C_2C_3O_4O_5$ and O_1, is very nearly in the plane of the paper. It is remarkable that all the six hydrogen bonds formed by this group also lie approximately in this plane. The same applies to the half $C'_2C'_3O'_4O'_5$ and O'_1, and thus all the hydrogen bonds in the structure lie approximately in planes perpendicular to the b axis and separated by a distance $\frac{1}{2}b$. The other half of the molecule is bonded to the surrounding molecules by four hydrogen bonds, all except one of which (O_7–O_5) are also in the plane of this half. This attempt at planarity of the molecule and its external bonds is also seen in oxalic acid dihydrate and thus appears to have some significance.

The methods described in this paper cannot distinguish between the d- and l-forms of an optically active compound, since parameters derived from those given by the operation of a centre of symmetry would give the same intensities. According to Waser (1949) a distinction between the two enantiomorphous structures can be made in favourable cases if the face development of the crystal is taken into consideration, and he comes to the conclusion that the configuration given in the present paper is that of the d-form. His arguments, however, have been criticized by Turner & Lonsdale (1950). We hope to comment on this problem at another time.

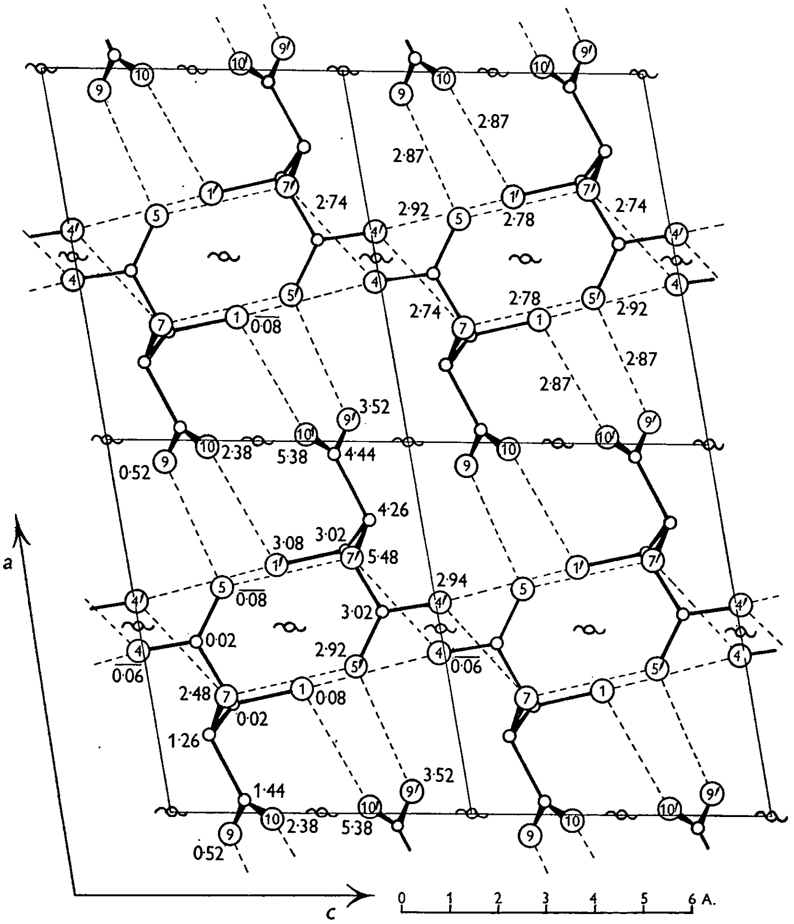

Fig. 8. The structure of tartaric acid projected down the b axis. In the lower left-hand unit cell the y co-ordinates (in Ångström units) are shown outside the circles representing the atoms. Probable hydrogen bonds are shown by dotted lines, and the hydrogen-bond lengths are shown in the upper right-hand cell.

One of us (F.S.) is indebted to the Carnegie Trust for the Universities of Scotland for a grant which enabled him to take part in this work.

References

Astbury, W. T. (1923). *Proc. Roy. Soc.* A, **102**, 506.
Beevers, C. A. & Hughes, W. (1941). *Proc. Roy. Soc.* A, **177**, 251.
Beevers, C. A. & Stern, F. (1948). *Nature, Lond.*, **162**, 854.
Booth, A. D. (1945). *Trans. Faraday Soc.* **41**, 434.
Buerger, M. J. (1946). *J. Appl. Phys.* **17**, 579.
Dunitz, J. D. & Robertson, J. M. (1947). *J. Chem. Soc.* p. 142.
Groth, P. (1906–19). *Chemische Krystallographie.* Leipzig: Engelmann.

Harker, D. (1936). *J. Chem. Phys.* **4**, 381.
Morrison, J. D. & Robertson, J. M. (1949). *J. Chem. Soc.* p. 980.
Reis, A. & Schneider, W. (1928). *Z. Krystallogr.* **69**, 62.
Robertson, J. M. & Woodward, I. (1936). *J. Chem. Soc.* p. 1817.
Turner, E. E. & Lonsdale, K. (1950). *J. Chem. Phys.* **18**, 156.
Waser, J. (1949). *J. Chem. Phys.* **17**, 498.
Wilson, A. J. C. (1942). *Nature, Lond.*, **150**, 152.
Winchell, A. N. (1943). *The Optical Properties of Organic Compounds.* University of Wisconsin.

Acta Cryst. (1950). **3**, 346

Ring Diffusion in Metals*

By Clarence Zener

Institute for the Study of Metals, University of Chicago, Chicago 37, *Ill., U.S.A.*

(*Received* 15 *December* 1949)

The concept of hole migration in metals as the mechanism of self-diffusion and of diffusion of substitution-solute atoms has arisen from the apparent failure of other reasonable mechanisms, such as direct interchange, to give heats of activation comparable to those observed. In the present paper it is pointed out that diffusion by direct interchange is only a special case of diffusion by the synchronized cyclic motion of a number of atoms, herein called ring diffusion. General arguments are presented demonstrating that a 4-ring has a lower potential-energy barrier for cyclic motion than has a 2-ring, which corresponds to direct interchange. These general arguments are supported by detailed calculations for the particular case of self-diffusion in copper. It is concluded that such ring diffusion is not excluded by energy considerations.

1. Introduction and results

In their study of the self-diffusion of copper, Huntington & Seitz (1942) found that in that metal an interchange of two neighboring atoms would require much more work than is represented by the observed heat of activation. They further found that this observed heat of activation is consistent with the concept that self-diffusion occurs by the mechanism of hole migration. That such migration does in fact occur in some appears (Smigelskas & Kirkendall, 1947) to be required by the Kirkendall experiment (R. Mehl, private communication). In the absence of any other mechanism of diffusion consistent with the observed heats of activation we would, therefore, be forced to accept hole migration as the primary mechanism responsible for self-diffusion in all metals as well as the diffusion of substitutional solute atoms. The purpose of this paper is to examine another possible mechanism.

Previous discussions of the mechanism of the diffusion of lattice atoms, as distinct from interstitial atoms, have started from the assumption that such diffusion must occur either by direct interchange of two neighboring atoms or by hole migration. While recognition has been indicated of the fact that disturbances involving the displacement or rotation of larger groups of atoms would also lead to diffusion (Le Claire, 1949, pp. 340–1), it has been implicitly assumed that the larger the group which participates in the elementary diffusion process the larger must be the work required to carry it over the free-energy barrier. The essential fallaciousness of this viewpoint is apparent once we recognize the smallness of the work per atom required to distort homogeneously a lattice to an unstable configuration midway between two stable configurations. Thus the author has shown (Zener, 1948, p. 36) that a work equivalent to only about 1600 cal./mole is required to strain homogeneously a copper lattice from one stable face-centered cubic (f.c.c.) configuration through an unstable body-centered cubic (b.c.c.) configuration on its way to a second f.c.c. configuration. This 1600 cal./mole is to be compared with the observed 60,000 cal./mole for the heat of activation for self-diffusion in copper. It is thereby apparent that the most appropriate region for an elementary diffusion act will be the most appropriate because of the smallness of its interaction with the surrounding lattice during the elementary diffusion act rather than because of the smallness of its size *per se*.

The interchange process discussed by Huntington & Seitz is represented in Fig. 1 as the rotation of a two-atom ring, hereafter abbreviated as a 2-ring. During this rotation the distance between the two-ring atoms, as well as the positions of the atoms in the surrounding lattice, must be regarded as adjusting themselves so as to minimize the work necessary to rotate the ring to its position of maximum free energy at the angle of $\frac{1}{2}\pi$. A possible 3-ring and 4-ring for f.c.c. lattices are illustrated in Figs. 2 and 3. These rings have been drawn so that each ring atom jumps into a nearest-neighbor position. It is anticipated that this nearest-neighbor requirement will be satisfied by that ring having the

---

* This research has been supported in part by the Office of Naval Research under Contract No. N6ori-20-IV, NR 019 302.